Journal of Alloys and Compounds, *197* (1993) 83–86
JALCOM 626

New ternary iron chalcogenides $A_9Fe_2X_7$ (A≡K, Rb, Cs; X≡S, Se): synthesis, crystal structure and magnetic properties

W. Bronger and U. Ruschewitz
Institut für Anorganische Chemie der Technischen Hochschule Aachen, Professor-Pirlet-Str. 1, W-5100 Aachen (Germany)

(Received December 28, 1992)

Abstract

The ternary iron chalcogenides $A_9Fe_2X_7$ with A≡K, Rb, Cs and X≡S, Se were synthesized by reaction of alkali carbonates with iron and the respective chalcogen in a stream of hydrogen. The crystal structures of the potassium and rubidium compounds were determined by single-crystal diffractometer data (spacegroup $P2_13$, $Z=4$). The atomic arrangement of the isotypic compounds is characterized by isolated trigonal nearly planar $[FeX_3]$ and tetrahedral $[FeX_4]$ units. The structure corresponds to that of $K_9Ni_2O_7$. The magnetic susceptibilities of $K_9Fe_2S_7$ reveal Curie–Weiss behaviour. The moment is due to a high spin state of both Fe^{3+} and Fe^{2+}. Magnetic ordering occurs below 6 K. Mössbauer experiments prove that the Fe^{3+} ions must be assigned to the tetrahedral coordination and the Fe^{2+} ions to the trigonal planar coordination.

1. Introduction

In 1986, Klepp and Bronger [1] prepared the ternary iron chalcogenide Na_5FeS_4, the structure of which is characterized by isolated $[FeS_4]^{5-}$ tetrahedra. In addition, the properties of Na_6FeS_4 and Na_6FeSe_4, two chalcogenides with isolated $[FeX_4]^{6-}$ tetrahedra, have recently been reported [2]. New ternary iron chalcogenides of the heavy alkali metals with isolated $[FeX_n]$ units ($n=3,4$) and the general composition $A_9Fe_2X_7$ (A≡K, Rb, Cs; X≡S, Se) are investigated in this study.

2. Syntheses

The chalcogenides $A_9Fe_2X_7$ were prepared from alkali carbonates, iron and the respective chalcogen. For the synthesis of $Cs_9Fe_2S_7$ and $Cs_9Fe_2Se_7$ caesium carbonate (Fa. Ventron, "ultrapure XT2") was dried for 24 h in a stream of hydrogen at 375 K. The reactants were weighed out according to the composition of the desired products and mixed. A corundum container and a quartz reaction tube were used. The mixtures were heated to 850–950 K for about 20 h in a stream of hydrogen and then cooled in an argon atmosphere.

The ternary sulphides are red; the colour darkens from the potassium to the caesium compound. The selenides are black. All compounds are sensitive to air and moisture, *e.g.* the sulphides change from red to black with a smell of H_2S when exposed to air.

3. Crystal structure

X-Ray investigations on powdered samples (Guinier method, Cu $K\alpha_1$ radiation) led to cubic unit cells. The cell parameters are listed in Table 1.

Single crystals of the potassium and rubidium compounds could be isolated from the solidified melts. Their crystal structures were solved from X-ray diffraction data. We failed to isolate single crystals of $Cs_9Fe_2S_7$, but the X-ray powder data suggest that it is isotypic with the other compounds. Single crystals of $Cs_9Fe_2Se_7$ could be isolated, but their structure determination led to negative values for some temperature coefficients caused by strong absorption effects. Nevertheless, the available structural data show that it is also isotypic with the other compounds.

The single-crystal X-ray diffraction data were collected on a four-circle diffractometer (Fa. Enraf-Nonius, CAD 4, graphite monochromator). Absorption effects were corrected by the ψ scan method. The anomalous

TABLE 1. $A_9Fe_2X_7$: cell parameters

Compound	*a* (pm)	Compound	*a* (pm)
$K_9Fe_2S_7$	1266.3(1)	$K_9Fe_2Se_7$	1311.8(1)
$Rb_9Fe_2S_7$	1311.0(1)	$Rb_9Fe_2Se_7$	1357.0(1)
$Cs_9Fe_2S_7$	1364.3(1)	$Cs_9Fe_2Se_7$	1408.7(4)

0925-8388/93/$6.00

dispersion was taken into account. The crystal data of the potassium and rubidium compounds are given in Table 2.

The structure of the isotypic chalcogenides is characterized by isolated trigonal nearly planar [FeX_3] units and by slightly trigonally distorted [FeX_4] tetrahedra. The atomic arrangement corresponds to that of $K_9Ni_2O_7$ [3]. Figure 1 shows a projection of the crystal structure of $K_9Fe_2S_7$ along [001]. Table 3 lists a few selected interatomic distances and bond angles of the compounds under discussion.

So far we have failed to synthesize the sodium compounds. However, preliminary tests show that mixed crystals exist with the composition $K_{9-x}Na_xFe_2S_7$ ($0 \leqslant x \leqslant 2.7$): single crystals have not yet been isolated. In the series $K_9Fe_2S_{7-x}Se_x$ the investigation of a single crystal with the composition $K_9Fe_2S_4Se_3$ shows no ordering of the chalcogen atoms.

TABLE 2. $A_9Fe_2X_7$: atomic positional and thermal parameters U_{ij} (pm^2), R values, radiation used, number (n) of independent reflections, θ range and size (s) of the crystals (mm)

Atom	x	y	z	U_{11}	U_{22}	U_{33}	U_{12}	U_{13}	U_{23}
$K_9Fe_2S_7$: $R=0.021$, Mo Kα, $n=812$ with $I \geqslant 3\sigma(I)$, $0° \leqslant \theta \leqslant 30°$, $s=0.20\times0.13\times0.25$									
K(1)	0.8330(1)	0.0017(1)	0.2992(1)	173(4)	183(4)	233(5)	19(4)	−4(5)	3(5)
K(2)	0.1762(1)	0.0420(1)	0.7926(1)	251(5)	224(5)	305(6)	8(5)	12(5)	18(5)
K(3)	0.4155(1)	x	x	315(5)	U_{11}	U_{11}	−58(5)	U_{12}	U_{12}
K(4)	0.2390(1)	x	x	202(4)	U_{11}	U_{11}	10(4)	U_{12}	U_{12}
K(5)	0.0594(1)	x	x	216(4)	U_{11}	U_{11}	−19(5)	U_{12}	U_{12}
Fe(1)	0.5708(1)	x	x	118(2)	U_{11}	U_{11}	4(3)	U_{12}	U_{12}
Fe(2)	0.9001(1)	x	x	112(2)	U_{11}	U_{11}	−4(3)	U_{12}	U_{12}
S(1)	0.9122(1)	0.0687(1)	0.8334(1)	177(5)	141(5)	209(5)	−29(5)	−24(5)	49(5)
S(2)	0.0757(1)	0.0610(1)	0.3108(1)	199(5)	228(5)	192(5)	−64(5)	−47(5)	93(5)
S(3)	0.7925(6)	x	x	159(4)	U_{11}	U_{11}	−20(5)	U_{12}	U_{12}
$Rb_9Fe_2S_7$: $R=0.038$, Mo Kα, $n=695$ with $I \geqslant 3\sigma(I)$, $0° \leqslant \theta \leqslant 35°$, $s=0.20\times0.2\times0.25$									
Rb(1)	0.8338(2)	0.0012(2)	0.2965(2)	250(10)	141(8)	190(9)	−10(10)	0(10)	−40(10)
Rb(2)	0.1747(2)	0.0426(2)	0.7913(2)	320(10)	230(10)	220(10)	−20(10)	10(10)	20(10)
Rb(3)	0.4178(2)	x	x	310(10)	U_{11}	U_{11}	−70(10)	U_{12}	U_{12}
Rb(4)	0.2385(2)	x	x	190(8)	U_{11}	U_{11}	15(9)	U_{12}	U_{12}
Rb(5)	0.0585(2)	x	x	195(8)	U_{11}	U_{11}	−30(10)	U_{12}	U_{12}
Fe(1)	0.5728(3)	x	x	120(10)	U_{11}	U_{11}	30(10)	U_{12}	U_{12}
Fe(2)	0.9000(2)	x	x	100(10)	U_{11}	U_{11}	0(10)	U_{12}	U_{12}
S(1)	0.9121(4)	0.0626(4)	0.8333(5)	190(30)	100(20)	170(30)	50(20)	40(30)	110(20)
S(2)	0.0785(5)	0.0549(5)	0.3127(4)	190(30)	120(30)	230(30)	−100(20)	−50(30)	10(20)
S(3)	0.7954(4)	x	x	140(20)	U_{11}	U_{11}	−20(20)	U_{12}	U_{12}
$K_9Fe_2Se_7$: $R=0.049$, Mo Kα, $n=575$ with $I \geqslant 3.5\sigma(I)$, $0° \leqslant \theta \leqslant 30°$, $s=0.18\times0.18\times0.09$									
K(1)	0.8315(6)	0.0011(5)	0.3004(6)	130(30)	280(40)	160(30)	−20(3)	40(30)	−10(30)
K(2)	0.1784(6)	0.0422(5)	0.7952(7)	270(40)	140(30)	360(40)	70(30)	0(40)	−20(30)
K(3)	0.4180(5)	x	x	340(30)	U_{11}	U_{11}	−130(40)	U_{12}	U_{12}
K(4)	0.2413(6)	x	x	230(30)	U_{11}	U_{11}	20(30)	U_{12}	U_{12}
K(5)	0.0591(6)	x	x	300(30)	U_{11}	U_{11}	−80(30)	U_{12}	U_{12}
Fe(1)	0.5703(3)	x	x	140(10)	U_{11}	U_{11}	0(20)	U_{12}	U_{12}
Fe(2)	0.8990(3)	x	x	100(10)	U_{11}	U_{11}	−10(20)	U_{12}	U_{12}
Se(1)	0.9135(2)	0.0695(2)	0.8308(2)	240(10)	180(10)	120(10)	−20(10)	−50(10)	30(10)
Se(2)	0.0751(3)	0.0625(3)	0.3086(2)	180(10)	180(10)	220(10)	−60(10)	70(10)	−70(10)
Se(3)	0.7902(2)	x	x	150(10)	U_{11}	U_{11}	−20(10)	U_{12}	U_{12}
$Rb_9Fe_2Se_7$: $R=0.046$, Ag Kα, $n=380$ with $I \geqslant 3.5\sigma(I)$, $0° \leqslant \theta \leqslant 24°$, $s=0.13\times0.15\times0.10$									
Rb(1)	0.8319(4)	0.0000(4)	0.2998(4)	320(30)	160(20)	160(20)	−20(30)	0(30)	−20(30)
Rb(2)	0.1769(4)	0.0421(4)	0.7946(5)	250(30)	270(30)	160(30)	−10(30)	−10(30)	−30(30)
Rb(3)	0.4206(4)	x	x	300(20)	U_{11}	U_{11}	−150(30)	U_{12}	U_{12}
Rb(4)	0.2398(4)	x	x	180(20)	U_{11}	U_{11}	50(30)	U_{12}	U_{12}
Rb(5)	0.0567(4)	x	x	180(20)	U_{11}	U_{11}	−20(30)	U_{12}	U_{12}
Fe(1)	0.5730(6)	x	x	150(30)	U_{11}	U_{11}	−40(40)	U_{12}	U_{12}
Fe(2)	0.8995(6)	x	x	100(30)	U_{11}	U_{11}	−20(40)	U_{12}	U_{12}
Se(1)	0.9139(4)	0.0636(4)	0.8316(4)	220(30)	170(30)	150(30)	30(30)	−30(30)	110(30)
Se(2)	0.0769(4)	0.0558(4)	0.3096(4)	150(30)	160(20)	110(20)	−50(30)	110(30)	−60(30)
Se(3)	0.7919(4)	x	x	90(20)	U_{11}	U_{11}	−30(20)	U_{12}	U_{12}

TABLE 3. $A_9Fe_2X_7$: selected interatomic distances (pm) and bond angles (°)

$K_9Fe_2S_7$					
K(1)–S(3)	305.3(2)	K(2)–S(2)	329.4(2)	K(3)–S(1)	315.8(2) (3×)
K(1)–S(1)	313.1(2)	K(2)–S(1)	333.5(2)	K(4)–S(2)	319.1(2) (3×)
K(1)–S(2)	316.7(2)	K(2)–S(3)	337.4(2)	K(4)–S(1)	340.3(2) (3×)
K(1)–S(2)	318.7(2)	K(2)–S(1)	340.0(2)	K(5)–S(2)	319.0(2) (3×)
K(1)–S(1)	325.9(2)	K(2)–S(2)	341.0(2)	K(5)–S(1)	341.8(2) (3×)
Fe(1)–S(2)	224.4(1) (3×)	S(2)–Fe(1)–S(2)	119.92(3) (3×)		
Fe(2)–S(1)	230.1(1) (3×)	S(1)–Fe(2)–S(1)	107.66(4) (3×)		
Fe(2)–S(3)	236.0(1)	S(1)–Fe(2)–S(3)	111.23(5) (3×)		
Fe(1)–Fe(2)	635.4(1) (3×)				
$Rb_9Fe_2S_7$					
Rb(1)–S(3)	315.9(6)	Rb(2)–S(2)	348.6(7)	Rb(3)–S(1)	330.3(7) (3×)
Rb(1)–S(1)	328.1(6)	Rb(2)–S(1)	349.2(7)	Rb(4)–S(2)	333.8(7) (3×)
Rb(1)–S(2)	329.1(7)	Rb(2)–S(3)	352.6(6)	Rb(4)–S(1)	358.7(6) (3×)
Rb(1)–S(2)	330.5(6)	Rb(2)–S(1)	349.6(6)	Rb(5)–S(2)	334.3(6) (3×)
Rb(1)–S(1)	336.5(6)	Rb(2)–S(2)	349.0(7)	Rb(5)–S(1)	352.2(7) (3×)
Fe(1)–S(2)	225.0(7) (3×)	S(2)–Fe(1)–S(2)	119.9(2) (3×)		
Fe(2)–S(1)	231.0(7) (3×)	S(1)–Fe(2)–S(1)	108.2(2) (3×)		
Fe(2)–S(3)	237.5(6)	S(1)–Fe(2)–S(3)	110.7(2) (3×)		
Fe(1)–Fe(2)	660.9(5) (3×)				
$K_9Fe_2Se_7$					
K(1)–Se(3)	317.2(7)	K(2)–Se(2)	342.3(10)	K(3)–Se(1)	326.8(7) (3×)
K(1)–Se(1)	324.0(8)	K(2)–Se(1)	348.4(8)	K(4)–Se(2)	332.2(9) (3×)
K(1)–Se(2)	329.7(9)	K(2)–Se(3)	346.5(7)	K(4)–Se(1)	348.7(8) (3×)
K(1)–Se(2)	331.3(8)	K(2)–Se(1)	352.4(8)	K(5)–Se(2)	328.0(8) (3×)
K(1)–Se(1)	336.8(8)	K(2)–Se(2)	351.8(9)	K(5)–Se(1)	355.5(8) (3×)
Fe(1)–Se(2)	235.9(5) (3×)	Se(2)–Fe(1)–Se(2)	120.0(2) (3×)		
Fe(2)–Se(1)	241.6(5) (3×)	Se(1)–Fe(2)–Se(1)	107.4(2) (3×)		
Fe(2)–Se(3)	247.2(5)	Se(1)–Fe(2)–Se(3)	111.5(2) (3×)		
Fe(1)–Fe(2)	656.6(6) (3×)				
$Rb_9Fe_2Se_7$					
Rb(1)–Se(3)	328.8(8)	Rb(2)–Se(2)	360.1(8)	Rb(3)–Se(1)	343.0(8) (3×)
Rb(1)–Se(1)	341.2(8)	Rb(2)–Se(1)	361.6(8)	Rb(4)–Se(2)	346.7(8) (3×)
Rb(1)–Se(2)	341.2(8)	Rb(2)–Se(3)	361.2(8)	Rb(4)–Se(1)	369.3(8) (3×)
Rb(1)–Se(2)	343.5(8)	Rb(2)–Se(1)	362.6(8)	Rb(5)–Se(2)	344.3(8) (3×)
Rb(1)–Se(1)	347.2(8)	Rb(2)–Se(2)	362.5(9)	Rb(5)–Se(1)	361.9(8) (3×)
Fe(1)–Se(2)	236.6(10) (3×)	Se(2)–Fe(1)–Se(2)	119.9(3) (3×)		
Fe(2)–Se(1)	241.8(10) (3×)	Se(1)–Fe(2)–Se(1)	107.9(3) (3×)		
Fe(2)–Se(3)	252.9(10)	Se(1)–Fe(2)–Se(3)	111.9(4) (3×)		
Fe(1)–Fe(2)	684.1(12) (3×)				

4. Magnetic properties

In order to characterize the magnetic properties of $K_9Fe_2S_7$ the susceptibilities were determined by the Faraday method in the temperature range 3.3–296.1 K [4]. A sample of 5.245 mg was sealed in an ampoule made from synthetic quartz (Suprasil, Fa. Heraeus). The susceptibilities were measured at five different field strengths from 0.1 to 1.4 T for each temperature. Throughout the whole temperature range no dependence on field strength was found so that the mean value of the five susceptibilities could be used. The diamagnetism of the core was corrected according to ref. 5. Figure 2 shows the $1/\chi_{mol}$ *vs.* T plot. The inset displays the low temperature range enlarged. The susceptibilities are referred to 1 formula unit. Curie–Weiss behaviour can be observed down to low temperatures. Below 6 K magnetic ordering obviously occurs. The negative value of $\theta = -18.0(3)$ K indicates antiferromagnetic interactions.

The calculated magnetic moment of 7.88(3) μ_B is due to a high spin state of both Fe^{3+} and Fe^{2+} according to the equation $\mu^2 = \mu^2(Fe^{2+}) + \mu^2(Fe^{3+})$. Assuming a spin-only value for Fe^{3+} ($\mu = 5.92$ μ_B), a magnetic moment of 5.21 μ_B is calculated for Fe^{2+}. This is in agreement with reported results [2]. For the other

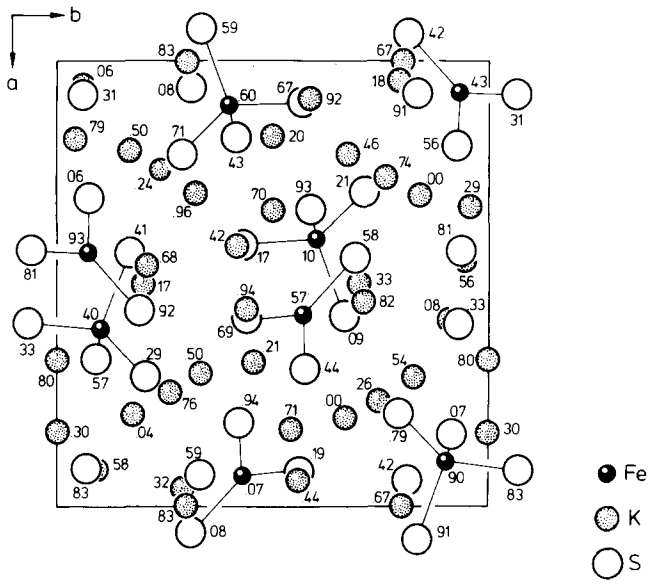

Fig. 1. $K_9Fe_2S_7$: atomic arrangement in a projection along [001].

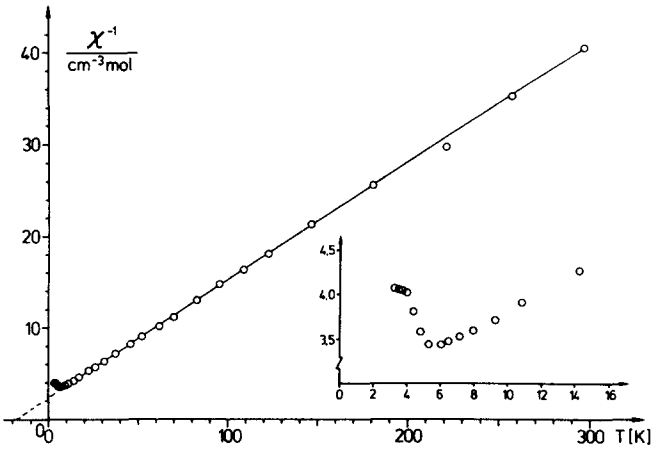

Fig. 2. $K_9Fe_2S_7$: $1/\chi_{mol}$ *vs.* T plot.

compounds analogous results were obtained. For $K_9Ni_2O_7$ [3] a magnetic moment of 5.1 μ_B was found. It was interpreted in terms of a high spin Ni^{3+} and a low spin diamagnetic Ni^{2+}. We assume that Ni^{2+} also adopts a high spin state as is the case with Fe^{2+} in $K_9Fe_2S_7$. Calculations in a simplified angular overlap model show a very small crystal field splitting of a trigonal planar environment [6] comparable with a tetrahedral ligand field. According to the equation $\mu^2 = \mu^2(Ni^{3+}) + \mu^2(Ni^{2+})$, and assuming a spin-only value for both Ni^{2+} and Ni^{3+}, a magnetic moment of 4.8 μ_B is calculated. The difference from the determined value may be interpreted in terms of spin–orbit coupling.

5. Mössbauer experiments

The Curie–Weiss behaviour indicates isolated paramagnetic centres. Therefore it was interesting to determine how the Fe^{3+} and Fe^{2+} ions are distributed in the different chalcogen environments. MAPLE calculations for $K_9Fe_2S_7$ according to ref. 3 point to $[FeS_3]^{4-}$ and $[FeS_4]^{5-}$ units. An examination of the Fe–S distances compared with other iron sulphides indicates the same distribution. Mössbauer experiments confirm these assumptions. Table 4 shows the results of Mössbauer measurements on different alkali metal iron sulphides.

TABLE 4. Mössbauer measurements on different alkali metal iron sulphides (room temperature; source: $^{57}Co/Rh$ at 300 K; IS relative to iron metal)

Compound	IS (mm s^{-1})	QS (mm s^{-1})
$K_9Fe_2S_7$	0.15	0
	0.39	0.20
Na_5FeS_4	0.18	0
Na_6FeS_4	0.66	0

IS, isomeric shift; QS, quadrupole splitting.

The isomeric shift (IS) in the Mössbauer experiments is very sensitive to the oxidation state and coordination number of a Mössbauer isotope. Therefore Na_5FeS_4 and Na_6FeS_4 were measured as reference compounds. The good agreement between the isomeric shift of the first Mössbauer peak of $K_9Fe_2S_7$ and that of Na_5FeS_4 confirms that Fe^{3+} has a tetrahedral environment. The quadrupole splitting (QS) of the second Mössbauer peak of $K_9Fe_2S_7$ points to an asymmetry of the ligand field which is due to a trigonal planar $[FeS_3]^{4-}$ unit.

Acknowledgments

We wish to thank Dr. D. Schmitz and Dr. P. Müller for help and discussions and Dr. C. Sauer for the Mössbauer experiments. We are also grateful to the Deutsche Forschungsgemeinschaft and the Fonds der Chemischen Industrie for financial support.

References

1 K. O. Klepp and W. Bronger, *Z. Anorg. Allg. Chem., 532* (1986) 23.
2 W. Bronger, H. Balk-Hardtdegen and U. Ruschewitz, *Z. Anorg. Allg. Chem., 616* (1992) 14.
3 H. Zentgraf and R. Hoppe, *Z. Anorg. Allg. Chem., 462* (1980) 80.
4 H. Lueken and W. Rohne, *Z. Anorg. Allg. Chem., 418* (1975) 103.
5 P. W. Selwood, *Magnetochemistry,* Interscience, New York 1964.
6 E. Larsen and G. N. La Mar, *Chem. Educ., 51* (10) (1974) 633.